

SUPPORTING INFORMATION FOR MANUSCRIPT

Study of the thermal processes in molecular crystals of peptides by means of NMR Crystallography

Tomasz Pawlak, Piotr Paluch, Katarzyna Trzeciak-Karlikowska, Agata Jeziorna and M. J.
Potrzebowski.

1) Polish Academy of Sciences, Centre of Molecular and Macromolecular Studies, Sienkiewicza 112,
90-363 Lodz, Poland.

EXPERIMENTAL – 2D PASS NMR Spectroscopy

A $5\text{-}\pi$ pulse 2D PASS scheme and 1000 and 2000 Hz sample spinning speeds were used in the 2D experiments on a BRUKER Avance III 400 spectrometer at a frequency of 100.613 MHz for ^{13}C equipped with a MAS probe head using 4 mm ZrO_2 rotors. The π -pulse length was 8 μs . Sixteen t_1 increments using the timings described by Levitt and co-workers were used in the 2D PASS experiments.¹ For each increment, 360 scans were accumulated. Because the pulse positions in the t_1 set return to their original positions after a full cycle and the t_1 -FID forms a full echo, the 16-point experimental t_1 data were replicated to 256 points. After the Fourier transformation in the direct dimension, the 2D spectrum was sheared to align all side bands with the center bands in the indirect dimension of the 2D spectrum. One-dimensional CSA spinning sideband patterns were obtained from t_1 slices taken at the isotropic chemical shifts in the t_2 dimension of the 2D spectrum. The magnitudes of the principal elements of the CSA tensor were obtained from the best-fit simulated spinning sideband pattern. Simulations of the spinning CSA sideband spectra were performed on a PC using the Topspin program.

RESULTS AND DISCUSSION

In this work, we employed the 2D PASS sequence for analysis of ^{13}C spectra.¹ This technique offers good sensitivity compared to other methods. In this paper, we reported ^{13}C δ_{ii} parameters for samples **1** and **2** analyzing 2D PASS spectra recorded at 2000 and 1000 Hz spinning rate. Figure S1 and S2 displays the example 2D PASS spectrum of **1** and **2** measured with a sample rotation 2000 Hz. The spectrum exhibits a complex pattern under slow sample spinning. Using proper data shearing (Figure S1B and S2B), it is possible to separate the spinning sidebands for each carbon and to use a calculational procedure to establish the ^{13}C δ_{ii} parameters. It is clear from such a presentation that the F2 projection corresponds to the infinite spinning speed spectrum, whereas F1 represents CSA. A similar procedure was employed to study **1**. The values of all ^{13}C δ_{ii} parameters for **1** and **2** are presented in Table S1 and S2.

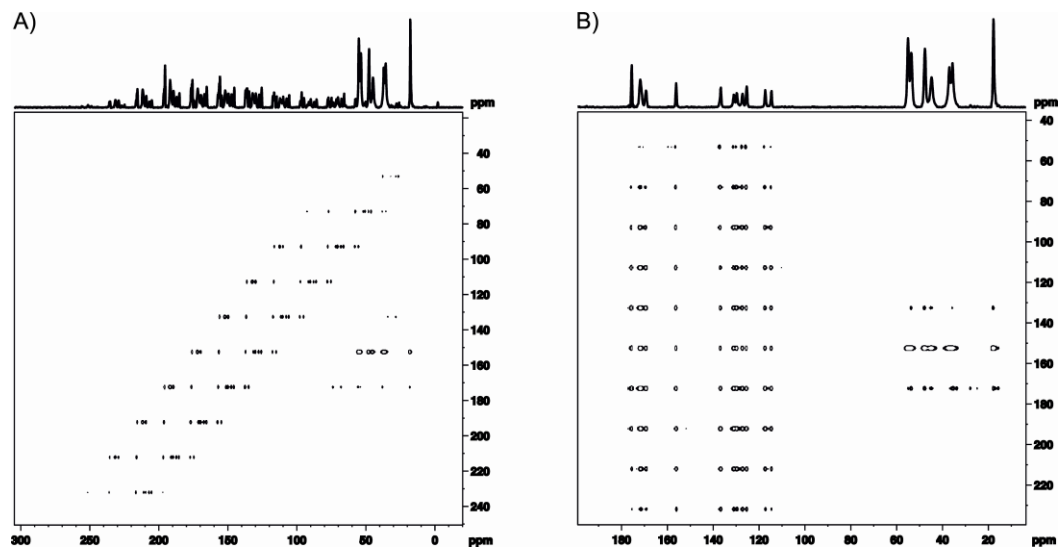


Figure S1. 2D PASS spectra for **1** recorded with a spinning rate of 2000 Hz (A) and the aliphatic part of spectrum after data shearing (B).

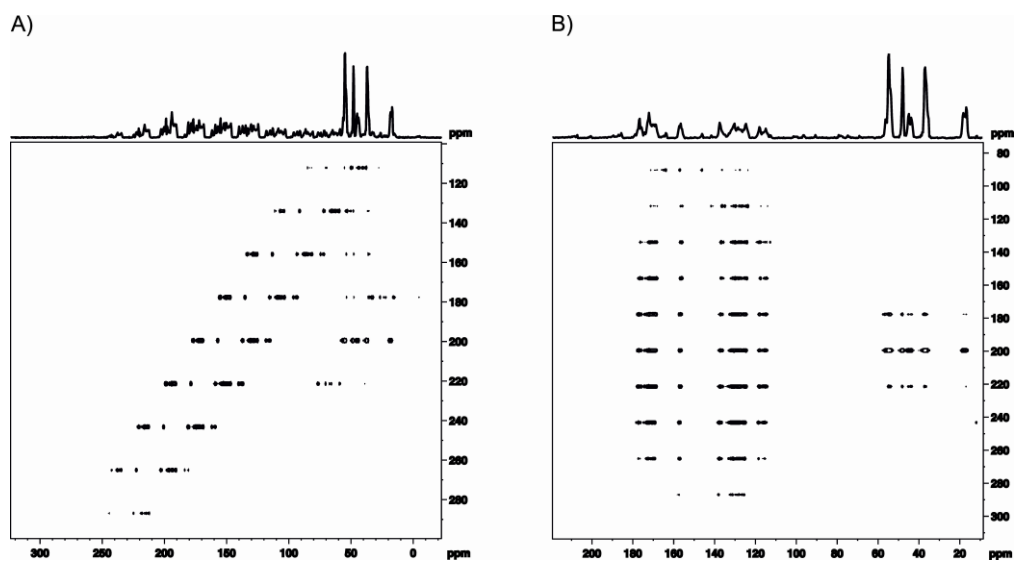


Figure S2. 2D PASS spectra for **2** recorded with a spinning rate of 2000 Hz (A) and the aliphatic part of spectrum after data shearing (B).

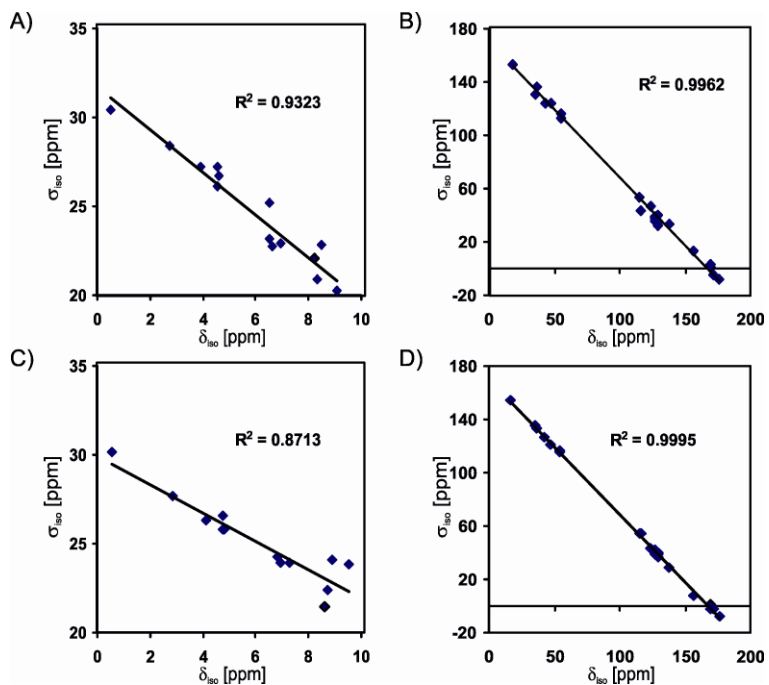


Figure S3. Correlation of the experimental isotropic chemical shift (δ_{iso}) versus the computed isotropic nuclear shielding (σ_{iso}) parameters (^1H –A, C and ^{13}C –B, D) for structure **2**. Calculations were done with increase (A and B) and decrease (C and D) unit cell dimensions of 10%.

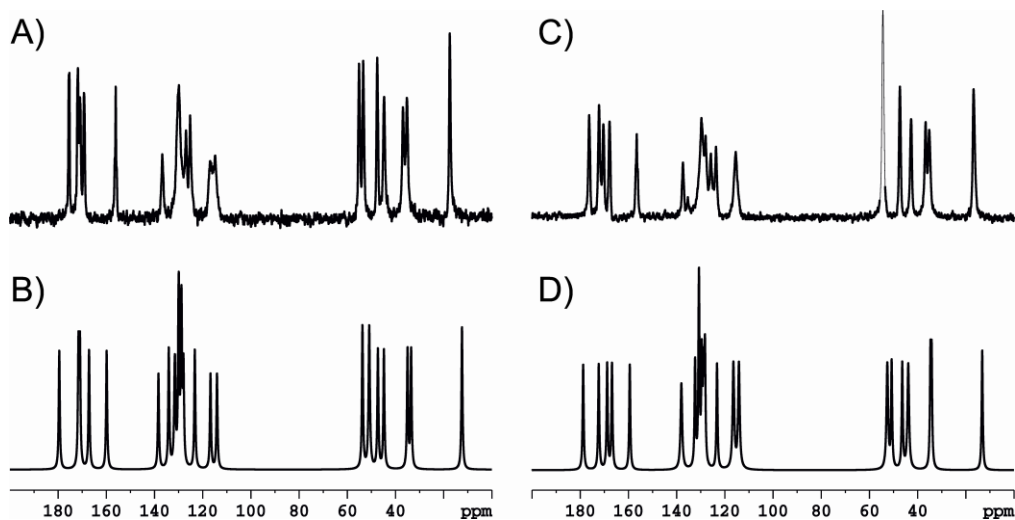


Figure S4. The ^{13}C NMR experimental spectrum of sample **1** and **2** recorded with spinning rate 55 kHz (Figure A and C respectively). The ^{13}C NMR simulated spectrum of sample **1** and **2** processed with line broadening equal to 70 Hz (GIPAW results).

Table S1. Experimental NMR chemical shift tensors [in ppm] for structure **1**.

Atom	δ_{iso}	δ_{11}	δ_{22}	δ_{33}	Ω^{a}	κ^{b}
C-10	168.9	243	173	91	152	0.08
C-11	54.8	69	58	37	32	0.30
C-12	35.8	46	44	17	29	0.85
C-13	125.3	221	150	5	216	0.34
C-14	129.7	239	142	8	231	0.16
C-15	114.4	194	124	25	169	0.17
C-16	155.8	247	157	63	184	0.02
C-17	117.2	198	134	20	178	0.28
C-18	130.9	223	149	21	202	0.27
C-20	171.5	246	185	84	162	0.25
C-21	47.4	66	52	24	42	0.33
C-22	17.8	32	29	-7	39	0.86
C-30	171.5	246	185	84	162	0.25
C-31	53.5	73	55	33	40	0.11
C-32	37.0	52	30	30	22	-0.95
C-33	136.6	229	166	15	214	0.41
C-34	130.9	223	149	21	202	0.27
C-35	127.2	224	153	5	219	0.35
C-36	127.2	224	153	5	219	0.35
C-37	127.2	224	153	5	219	0.35
C-38	130.9	223	149	21	202	0.27
C-40	175.2	236	176	114	122	0.02
C-41	44.4	66	50	17	49	0.34

^a Span is expressed as: $\Omega = \delta_{11} - \delta_{33}$

^b Skew is expressed as: $\kappa = (\delta_{22} - \delta_{\text{iso}})/\Omega$

Table S2. Experimental NMR chemical shift tensors [in ppm] for structure **2**.

Atom	δ_{iso}	δ_{11}	δ_{22}	δ_{33}	Ω^{a}	κ^{b}
C-10	169.2	249	169	90	159	0.00
C-11	54.3	72	47	44	28	-0.79
C-12	35.0	48	29	28	20	-0.90
C-13	123.7	218	143	10	208	0.28
C-14	129.5	222	143	25	197	0.21
C-15	115.1	197	126	23	174	0.19
C-16	156.7	245	164	61	185	0.12
C-17	116.3	191	133	25	166	0.30
C-18	129.5	222	143	25	197	0.21
C-20	169.8	251	171	87	163	0.02
C-21	47.2	68	46	29	39	-0.09
C-22	17.0	- ^c	- ^c	- ^c	- ^c	- ^c
C-30	171.7	243	184	88	155	0.24
C-31	54.3	72	47	44	28	-0.79
C-32	36.5	55	28	27	28	-0.91
C-33	137.5	230	168	14	216	0.42
C-34	129.5	222	141	26	196	0.17
C-35	127.1	226	145	10	216	0.25
C-36	127.1	226	145	10	216	0.25
C-37	127.1	226	145	10	216	0.25
C-38	129.5	222	143	25	197	0.21
C-40	176.1	238	172	118	120	-0.10
C-41	42.8	70	41	18	52	-0.10

^a Span is expressed as: $\Omega = \delta_{11} - \delta_{33}$

^b Skew is expressed as: $\kappa = (\delta_{22} - \delta_{\text{iso}})/\Omega$

^c Experimental data can not be obtained

Table S3. CASTEP calculations. NMR chemical shift tensors [in ppm] for structure **1** calculated using PBE0 functional with ultrasoft pseudopotential and GIPAW approach. Geometry (only hydrogen positions) was optimized with PBE0 functional and ultrasoft pseudopotential. Cut-off energy was: 550 eV. The chemical shifts were calculated from shielding parameters (σ_i) using the equations: $\delta_i = 171.0 - \sigma_i(\text{C})$.

Atom	δ_{iso}	δ_{11}	δ_{22}	δ_{33}	Ω^{a}	κ^{b}
C-10	168.4	243.4	171.9	89.9	153.5	0.07
C-11	53.6	65.2	55.3	40.4	24.8	0.20
C-12	36.3	51.7	46.1	11.2	40.5	0.73
C-13	124.7	220.2	148.6	5.3	214.9	0.33
C-14	132.4	233.3	152.3	11.5	221.9	0.27
C-15	115.7	201.8	130.9	14.5	187.3	0.24
C-16	161.1	243.4	174.5	65.5	178.0	0.23
C-17	118.8	201.4	140.8	14.2	187.2	0.35
C-18	129.8	231.0	130.3	28.1	203.0	0.01
C-20	170.6	244.3	176.1	91.3	153.0	0.11
C-21	45.7	64.0	50.0	23.2	40.8	0.31
C-22	14.3	30.8	18.1	-5.9	36.7	0.31
C-30	168.7	238.6	179.2	88.4	150.2	0.21
C-31	52.6	71.9	57.6	28.4	43.6	0.34
C-32	38.6	51.1	44.5	20.3	30.8	0.57
C-33	139.0	237.8	173.7	5.4	232.4	0.45
C-34	135.0	240.2	150.7	14.0	226.2	0.21
C-35	131.6	241.8	144.5	8.4	233.5	0.17
C-36	125.6	231.2	146.5	-0.9	232.2	0.27
C-37	130.7	236.5	150.9	4.7	231.8	0.26
C-38	132.0	238.8	137.7	19.6	219.2	0.08
C-40	162.6	226.2	168.9	92.8	133.4	0.14
C-41	43.1	64.3	47.8	17.3	47.0	0.30

^a Span is expressed as: $\Omega = \delta_{11} - \delta_{33}$

^b Skew is expressed as: $\kappa = (\delta_{22} - \delta_{\text{iso}})/\Omega$

Table S4. CASTEP calculations. NMR chemical shift tensors [in ppm] for structure **1** calculated using PBE0 functional with ultrasoft pseudopotential and GIPAW approach. Geometry (all positions) was optimized with PBE0 functional and ultrasoft pseudopotential. Cut-off energy was: 550 eV. The chemical shifts were calculated from shielding parameters (σ_i) using the equations: $\delta_i = 168.8 - \sigma_i(\text{C})$.

Atom	δ_{iso}	δ_{11}	δ_{22}	δ_{33}	Ω^{a}	κ^{b}
C-10	171.0	244.1	181.9	86.9	157.2	0.21
C-11	53.7	63.7	52.0	45.3	18.4	-0.28
C-12	33.5	47.7	41.0	11.9	35.8	0.63
C-13	123.3	219.1	147.2	3.6	215.5	0.33
C-14	130.1	234.3	145.7	10.4	224.0	0.21
C-15	114.4	199.0	131.7	12.4	186.6	0.28
C-16	159.9	243.3	174.0	62.3	181.1	0.23
C-17	116.8	200.7	137.8	12.0	188.7	0.33
C-18	129.9	232.3	137.0	20.3	212.0	0.10
C-20	167.2	244.3	167.6	89.8	154.5	0.01
C-21	47.3	69.2	45.6	27.0	42.2	-0.12
C-22	12.4	26.8	16.8	-6.5	33.3	0.40
C-30	171.6	240.3	186.2	88.4	151.9	0.29
C-31	50.9	72.9	54.1	25.7	47.2	0.20
C-32	35.0	47.4	41.1	16.7	30.7	0.59
C-33	138.4	238.0	173.4	3.7	234.3	0.45
C-34	134.1	240.0	151.3	10.9	229.2	0.23
C-35	128.8	237.3	144.3	4.8	232.5	0.20
C-36	128.0	235.1	151.5	-2.7	237.8	0.30
C-37	131.6	240.3	151.5	2.9	237.4	0.25
C-38	129.0	235.0	135.2	16.9	218.1	0.08
C-40	179.5	245.8	187.3	105.4	140.4	0.17
C-41	44.8	64.8	47.5	22.1	42.7	0.19

^a Span is expressed as: $\Omega = \delta_{11} - \delta_{33}$

^b Skew is expressed as: $\kappa = (\delta_{22} - \delta_{\text{iso}})/\Omega$

Table S5. CASTEP calculations. NMR chemical shift tensors [in ppm] for structure **2** calculated using PBE0 functional with ultrasoft pseudopotential and GIPAW approach. Geometry (all positions) was optimized with PBE0 functional and ultrasoft pseudopotential. Cut-off energy was: 550 eV. The chemical shifts were calculated from shielding parameters (σ_i) using the equations: $\delta_i = 168.5 - \sigma_i(\text{C})$.

Atom	δ_{iso}	δ_{11}	δ_{22}	δ_{33}	Ω^{a}	κ^{b}
C-10	166.9	245.3	165.8	89.8	155.5	-0.02
C-11	52.6	62.0	51.4	44.3	17.6	-0.20
C-12	34.2	49.6	40.7	12.5	37.0	0.52
C-13	123.3	219.2	147.2	3.4	215.8	0.33
C-14	130.8	234.6	148.4	9.3	225.3	0.23
C-15	114.2	199.2	131.0	12.5	186.8	0.27
C-16	159.5	243.2	173.1	62.2	181.0	0.23
C-17	116.5	200.0	137.4	12.1	187.9	0.33
C-18	129.6	231.5	134.9	22.3	209.2	0.08
C-20	168.9	243.9	172.4	90.4	153.5	0.07
C-21	46.4	68.3	45.4	25.5	42.9	-0.07
C-22	13.2	29.1	17.1	-6.4	35.5	0.32
C-30	172.4	239.7	188.7	88.9	150.8	0.32
C-31	50.8	72.2	55.3	24.8	47.4	0.29
C-32	34.7	46.6	40.3	17.2	29.4	0.57
C-33	138.1	236.9	173.7	3.8	233.1	0.46
C-34	132.4	238.7	147.6	11.0	227.7	0.20
C-35	128.3	237.8	142.5	4.6	233.1	0.18
C-36	128.2	236.1	151.1	-2.5	238.7	0.29
C-37	130.8	240.1	150.1	2.4	237.7	0.24
C-38	128.9	234.5	135.1	17.2	217.4	0.08
C-40	178.8	245.0	187.4	104.0	141.0	0.18
C-41	43.9	63.2	48.0	20.6	42.6	0.29

^a Span is expressed as: $\Omega = \delta_{11} - \delta_{33}$

^b Skew is expressed as: $\kappa = (\delta_{22} - \delta_{\text{iso}})/\Omega$

Table S6. Quantum Espresso calculations. NMR chemical shift tensors [in ppm] for structure **1** calculated using PBE0 functional with of the norm-conserving Troullier–Martins pseudopotential and GIPAW approach. Geometry (all positions) was optimized with PBE0 functional and norm-conserving Troullier–Martins pseudopotential. Cut-off energy was: 60 Ryd. The chemical shifts were calculated from shielding parameters (σ_i) using the equations: $\delta_i = 163.1 - \sigma_i(\text{C})$.

Atom	δ_{iso}	δ_{11}	δ_{22}	δ_{33}	Ω^a	κ^b
C-10	175.3	250.8	189.1	86.1	164.7	0.25
C-11	51.7	62.2	50.5	42.5	19.7	-0.18
C-12	30.7	45.6	38.0	8.6	36.9	0.59
C-13	123.1	221.2	147.8	0.3	221.0	0.34
C-14	129.7	234.6	148.7	5.9	228.7	0.25
C-15	112.7	199.9	131.4	6.9	193.0	0.29
C-16	161.3	246.4	176.4	61.0	185.4	0.24
C-17	118.4	205.0	144.1	6.2	198.8	0.39
C-18	129.4	232.7	138.7	16.7	216.1	0.13
C-20	171.0	249.8	175.1	87.9	161.9	0.08
C-21	46.4	69.0	43.1	27.2	41.8	-0.24
C-22	10.6	25.9	15.8	-10.0	35.9	0.43
C-30	175.2	245.0	194.1	86.4	158.7	0.36
C-31	51.0	72.0	56.4	24.7	47.3	0.34
C-32	32.8	44.6	38.6	15.3	29.3	0.59
C-33	138.1	240.2	173.8	0.3	239.8	0.45
C-34	131.7	240.4	148.0	6.6	233.8	0.21
C-35	127.2	239.1	142.7	-0.3	239.4	0.19
C-36	127.1	237.2	152.4	-8.4	245.6	0.31
C-37	130.9	242.1	153.2	-2.8	244.9	0.27
C-38	127.1	235.1	135.7	10.6	224.5	0.11
C-40	186.3	256.2	197.1	105.5	150.7	0.22
C-41	43.5	63.8	46.3	20.4	43.4	0.19

^a Span is expressed as: $\Omega = \delta_{11} - \delta_{33}$

^b Skew is expressed as: $\kappa = (\delta_{22} - \delta_{\text{iso}})/\Omega$

Table S7. Quantum Espresso calculations. NMR chemical shift tensors [in ppm] for structure **1** calculated using PBE0 functional with of the norm-conserving Troullier–Martins pseudopotential and GIPAW approach. Geometry (all positions) was optimized with PBE0 functional and norm-conserving Troullier–Martins pseudopotential. The van der Waals (vdW) interactions were included using vdW-DF exchange-correlation Cut-off energy was: 60 Ryd. The chemical shifts were calculated from shielding parameters (σ_i) using the equations: $\delta_i = 164.1 - \sigma_i(\text{C})$.

Atom	δ_{iso}	δ_{11}	δ_{22}	δ_{33}	Ω^a	κ^b
C-10	175.6	242.8	199.1	85.0	157.8	0.45
C-11	52.4	62.0	51.1	44.2	17.8	-0.23
C-12	31.6	46.7	40.5	7.4	39.3	0.68
C-13	123.5	221.8	148.1	0.6	221.2	0.33
C-14	130.6	234.2	149.5	8.2	226.1	0.25
C-15	113.6	199.7	130.8	10.3	189.4	0.27
C-16	161.4	246.6	178.0	59.6	187.0	0.27
C-17	119.0	204.0	145.0	8.0	196.1	0.40
C-18	127.3	229.2	133.1	19.6	209.7	0.08
C-20	169.3	244.5	175.9	87.6	156.8	0.13
C-21	46.1	67.2	44.0	27.3	39.9	-0.16
C-22	11.3	27.4	16.4	-10.0	37.5	0.41
C-30	173.0	236.8	196.7	85.5	151.3	0.47
C-31	50.6	70.0	58.5	23.3	46.7	0.51
C-32	34.4	47.4	39.7	16.2	31.2	0.51
C-33	137.6	240.4	172.4	0.0	240.3	0.43
C-34	132.8	240.3	148.5	9.7	230.6	0.20
C-35	128.0	238.7	144.0	1.4	237.2	0.20
C-36	127.2	236.4	151.5	-6.3	242.7	0.30
C-37	132.3	242.1	155.0	-0.4	242.5	0.28
C-38	127.6	234.2	136.0	12.6	221.6	0.11
C-40	183.9	253.5	193.8	104.4	149.0	0.20
C-41	41.8	64.2	42.5	18.8	45.5	0.05

^a Span is expressed as: $\Omega = \delta_{11} - \delta_{33}$

^b Skew is expressed as: $\kappa = (\delta_{22} - \delta_{\text{iso}})/\Omega$

Table S8. Quantum Espresso calculations. NMR chemical shift tensors [in ppm] for structure **2** calculated using PBE0 functional with of the norm-conserving Troullier–Martins pseudopotential and GIPAW approach. Geometry (all positions) was optimized with PBE0 functional and norm-conserving Troullier–Martins pseudopotential. Cut-off energy was: 60 Ryd. The chemical shifts were calculated from shielding parameters (σ_i) using the equations: $\delta_i = 163.1 - \sigma_i(\text{C})$.

Atom	δ_{iso}	δ_{11}	δ_{22}	δ_{33}	Ω^a	κ^b
C-10	172.5	252.9	176.6	87.8	165.1	0.08
C-11	52.5	63.0	53.2	41.3	21.8	0.09
C-12	29.2	42.9	37.8	7.0	35.8	0.71
C-13	124.4	222.6	149.7	1.0	221.6	0.34
C-14	130.2	235.9	149.9	4.9	231.1	0.26
C-15	113.9	202.6	131.1	8.1	194.6	0.26
C-16	161.3	246.4	176.2	61.3	185.1	0.24
C-17	117.2	203.5	141.3	6.8	196.7	0.37
C-18	128.1	232.4	133.3	18.7	213.7	0.07
C-20	172.8	249.5	180.2	88.8	160.7	0.14
C-21	45.2	67.7	43.9	24.1	43.5	-0.09
C-22	10.1	25.6	14.7	-9.9	35.5	0.39
C-30	174.9	244.5	192.6	87.4	157.1	0.34
C-31	51.0	72.2	57.1	23.8	48.3	0.37
C-32	31.7	44.0	36.9	14.1	29.9	0.53
C-33	137.5	239.9	172.3	0.5	239.4	0.43
C-34	131.8	240.2	148.3	6.8	233.3	0.21
C-35	127.4	239.2	143.0	0.0	239.2	0.20
C-36	127.2	237.4	152.2	-8.0	245.4	0.31
C-37	130.9	241.9	153.3	-2.4	244.3	0.27
C-38	127.1	234.7	135.1	11.3	223.4	0.11
C-40	184.1	262.2	183.2	106.8	155.5	-0.02
C-41	41.4	63.2	44.8	16.2	47.0	0.22

^a Span is expressed as: $\Omega = \delta_{11} - \delta_{33}$

^b Skew is expressed as: $\kappa = (\delta_{22} - \delta_{\text{iso}})/\Omega$

Table S9. Quantum Espresso calculations. NMR chemical shift tensors [in ppm] for structure **2** calculated using PBE0 functional with of the norm-conserving Troullier–Martins pseudopotential and GIPAW approach. Geometry (all positions) was optimized with PBE0 functional and norm-conserving Troullier–Martins pseudopotential. The van der Waals (vdW) interactions were included using vdW-DF exchange-correlation Cut-off energy was: 60 Ryd. The chemical shifts were calculated from shielding parameters (σ_i) using the equations: $\delta_i = 164.1 - \sigma_i(\text{C})$.

Atom	δ_{iso}	δ_{11}	δ_{22}	δ_{33}	Ω^a	κ^b
C-10	171.7	247.4	180.1	87.6	159.8	0.16
C-11	51.5	60.4	51.5	42.4	18.0	0.01
C-12	30.9	44.8	40.8	7.1	37.8	0.78
C-13	123.9	222.2	149.3	0.2	222.0	0.34
C-14	131.4	235.0	152.5	6.7	228.3	0.28
C-15	114.2	200.7	131.4	10.5	190.3	0.27
C-16	161.0	246.3	176.4	60.3	186.0	0.25
C-17	119.1	203.6	145.3	8.4	195.2	0.40
C-18	127.3	230.0	131.3	20.6	209.4	0.06
C-20	171.9	243.9	183.2	88.6	155.4	0.22
C-21	44.7	65.9	44.1	24.0	41.9	-0.04
C-22	11.0	28.5	14.8	-10.3	38.8	0.29
C-30	173.4	235.8	197.3	87.0	148.8	0.48
C-31	51.0	69.4	59.3	24.3	45.1	0.55
C-32	34.1	47.7	38.7	16.0	31.8	0.43
C-33	137.0	239.7	171.2	0.1	239.6	0.43
C-34	132.5	239.4	147.9	10.1	229.3	0.20
C-35	128.0	238.3	143.9	1.8	236.5	0.20
C-36	127.6	236.8	152.0	-6.0	242.8	0.30
C-37	132.2	242.2	154.5	-0.2	242.4	0.28
C-38	127.5	233.6	135.8	13.0	220.6	0.11
C-40	182.3	254.5	186.9	105.5	149.0	0.09
C-41	41.4	63.5	44.4	16.2	47.3	0.19

^a Span is expressed as: $\Omega = \delta_{11} - \delta_{33}$

^b Skew is expressed as: $\kappa = (\delta_{22} - \delta_{\text{iso}})/\Omega$

Coordinates for sample 2.

O	1.054070	7.161871	6.179545
O	4.440367	1.435661	3.551614
H	5.066213	0.772178	3.947614
N	2.609496	7.087253	8.704379
H	3.108864	7.985366	8.727247
H	3.023636	6.542297	9.539829
H	1.582723	7.236086	8.925057
C	2.290924	7.039977	6.250627
C	2.926433	6.343360	7.456541
H	4.021495	6.344707	7.365259
C	2.405152	4.901638	7.582887
H	2.711710	4.520600	8.569076
H	1.304745	4.930058	7.562115
C	2.943034	3.993963	6.508656
C	2.422902	3.989114	5.205743
H	1.575839	4.632393	4.959720
C	2.938376	3.149052	4.221269
H	2.515293	3.143799	3.216786
C	3.987092	2.272624	4.528465
C	4.522806	2.272624	5.822802
H	5.328395	1.582608	6.062727
C	4.003087	3.125481	6.791840
H	4.414770	3.095176	7.802993
O	4.552995	9.574439	3.848519
N	3.160327	7.439467	5.304267
H	4.170355	7.339797	5.477684
C	3.322255	9.402305	3.880344
C	2.733576	7.992639	4.023651
H	1.637792	8.052846	4.057000
C	3.190410	7.107726	2.864426

H	2.773226	6.098359	2.969048
H	4.286042	7.040246	2.846894
H	2.857103	7.527420	1.905870
O	0.978451	12.957986	4.785350
N	2.407551	10.387158	3.794207
H	1.406548	10.143504	3.827366
C	2.163836	12.549202	4.809934
C	2.757103	11.790089	3.618313
H	3.853271	11.852720	3.645754
C	2.217331	12.347840	2.284719
H	1.124124	12.227697	2.276905
H	2.430703	13.426573	2.268330
C	2.830284	11.678835	1.083569
C	2.394651	10.414500	0.657840
H	1.549260	9.940122	1.158081
C	3.012635	9.769739	-0.414104
H	2.660450	8.785155	-0.728541
C	4.065963	10.384195	-1.094813
H	4.557055	9.869544	-1.921687
C	4.482523	11.657958	-0.702433
H	5.302448	12.146075	-1.226495
C	3.871124	12.297601	0.376943
H	4.208238	13.291209	0.683376
O	4.425016	12.635942	8.223767
O	3.075647	14.134907	9.220437
N	2.939167	12.690626	5.891788
H	3.926480	12.420169	5.873874
C	3.389248	13.368656	8.255020
C	2.439429	13.376333	7.068926
H	1.479679	12.931991	7.376883
H	2.239861	14.431360	6.833574

¹ O. N. Antzutkin, S. C. Shekar, M. H. Levitt, *J. Magn. Reson. Ser. A*, 1995, **115**, 7.